Analysis of soil carbon transit times and age distributions using network theories

Stefano Manzoni,[1] Gabriel G. Katul,[1,2] and Amilcare Porporato[1]

Received 8 June 2009; revised 12 September 2009; accepted 21 September 2009; published 30 December 2009.

[1] The long-term soil carbon dynamics may be approximated by networks of linear compartments, permitting theoretical analysis of transit time (i.e., the total time spent by a molecule in the system) and age (the time elapsed since the molecule entered the system) distributions. We compute and compare these distributions for different network configurations, ranging from the simple individual compartment, to series and parallel linear compartments, feedback systems, and models assuming a continuous distribution of decay constants. We also derive the transit time and age distributions of some complex, widely used soil carbon models (the compartmental models CENTURY and Rothamsted, and the continuous-quality Q-Model), and discuss them in the context of long-term carbon sequestration in soils. We show how complex models including feedback loops and slow compartments have distributions with heavier tails than simpler models. Power law tails emerge when using continuous-quality models, indicating long retention times for an important fraction of soil carbon. The responsiveness of the soil system to changes in decay constants due to altered climatic conditions or plant species composition is found to be stronger when all compartments respond equally to the environmental change, and when the slower compartments are more sensitive than the faster ones or lose more carbon through microbial respiration.

Citation: Manzoni, S., G. G. Katul, and A. Porporato (2009), Analysis of soil carbon transit times and age distributions using network theories, *J. Geophys. Res.*, *114*, G04025, doi:10.1029/2009JG001070.

1. Introduction

[2] The long-term dynamics of soil and plant residue carbon (C) are receiving considerable interest because of the need to quantify long-term C sinks in soils under altered climatic conditions and following shifts in land use [*Lal*, 2008]. Two parameters are employed to define the soil effectiveness to retain C, transit time (sometimes referred to as residence time) and age of organic matter C (Figure 1). Transit time here is defined following *Eriksson* [1971] and *McGuire and McDonnell* [2006] as the time a soil organic matter (SOM) molecule remains in the soil since its deposition as plant residue, and until its release as mineralized products. The age is the time elapsed since the molecule entered the soil, and it is mathematically related to the transit time. According to this definition, the transit time is equivalent to the age at the time of exit.

[3] The transit time of SOM carbon depends on a number of processes acting at the yearly to decadal, or even longer timescales. In particular, the physical and chemical protection of SOM fractions, and variable microbial activity, may contribute to the different and possibly low decay rates that are observed [*Blanco-Canqui and Lal*, 2004; *von Luetzow et al.*, 2008]. Spatial heterogeneity also plays a role, since it mediates the relative importance of the different organic matter retention mechanisms. Hence, the transit time can be used as a single parameter that integrates a number of biochemical and physical processes characterizing SOM dynamics.

[4] Biogeochemical cycling is often described by means of mathematical models based on a number of interconnected compartments, each releasing C according to linear and nonlinear kinetic laws. Nonlinear kinetics may be preferred when describing short-term processes because the coupling of decomposer biomass and organic matter substrate is important [*Manzoni and Porporato*, 2007, 2009; *Schimel*, 2001]. However, for long-term studies (yearly timescale or longer), organic matter dynamics may be approximated by a system of compartments each exchanging C following first-order kinetics [*Baisden and Amundson*, 2003; *Manzoni and Porporato*, 2009]. At those timescales, the decomposer activity may be considered relatively constant, thereby making the amount of available substrate the predominant controlling factor of the C fluxes. The linear approximation is also often used to describe short-term dynamics where the decomposers' activity rapidly adapts to substrate availability and hence is never a limiting factor [*Manzoni and Porporato*, 2009]. Accordingly, soil is often regarded as a linear time-invariant input-output system, where the dynamics of the output (e.g., heterotrophic respiration) is computed as a function of the previous inputs

[1]Civil and Environmental Engineering Department, Duke University, Durham, North Carolina, USA.
[2]Nicholas School of the Environment, Duke University, Durham, North Carolina, USA.

Copyright 2009 by the American Geophysical Union.
0148-0227/09/2009JG001070$09.00

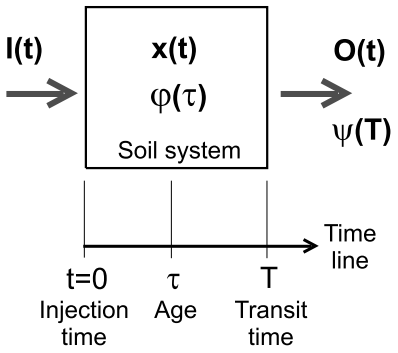

Figure 1. Schematic representation of a generic system with input $I(t)$, output $O(t)$, mass $x(t)$, transit time density distribution $\psi(T)$, and age density distribution $\varphi(\tau)$. Each molecule enters the system at age $\tau = 0$, and leaves at age equal to the transit time T.

of organic matter to the soil and a suitable "weighting function" that describes how much C remains in the soil of the past inputs at present time [*Bolin and Rodhe*, 1973; *Eriksson*, 1971]. Such a weighting function can be interpreted as the probability distribution of the times spent by each C molecule within the system, i.e., the transit time distribution, and can be used to transform a generic input into the output from the system [*Eriksson*, 1971; *Nir and Lewis*, 1975]. This overall transit time distribution results from the combination of the transit time distributions of the individual well mixed linear compartments making up the complex network of biogeochemical cycling, thereby carrying all (in the case of a linear system) the information on the system architecture.

[5] The mathematical theory behind linear input-output systems is well established, and has been used in climate studies [*Bolin*, 1981; *Enting*, 2007; *Thompson and Randerson*, 1999], hydrology [*Nash*, 1957; *Dingman*, 1994; *Rodriguez-Iturbe and Valdes*, 1979; *McGuire and McDonnell*, 2006], nutrient and contaminant transport [*Rinaldo et al.*, 2006; *Sardin et al.*, 1991], chemical engineering [*Aris*, 1989; *Nauman*, 2008], as well as in signal and electrical circuit theory [e.g., *Chen*, 2004]. Despite the fact that most long-term soil C models are linear [*Manzoni and Porporato*, 2009], there are only few applications of the theory to soil and ecosystem biogeochemistry. Notable exceptions are the linear analysis of organic matter cohorts [*Ågren and Bosatta*, 1996], of retention of C tracers in soils [*Balesdent*, 1987; *Ågren et al.*, 1996; *Bruun et al.*, 2004, 2005], and of the sensitivity of ecosystem C compartments to increased atmospheric carbon dioxide concentrations [*Emanuel et al.*, 1981; *Thompson and Randerson*, 1999]. In these studies, the theoretical relationships between the age and transit time distributions, as well as the sensitivity of C transit times to changes in model structure and kinetic constants, were not explicitly considered.

[6] In addition to the above applications, linear system theory is also useful to critically compare the variety of linear model structures that have been proposed and used in characterizing long-term SOM dynamics. The transit time distribution, which can be computed from the model compartmental organization, is especially suited to this goal. Directly computing the transit time distribution has also the advantage of retaining the relevant information on the long-term persistence of C in soils in an analytical compact formulation. For example, heavy-tailed transit time distributions hint at efficient C retention mechanisms resulting from low decomposition rates and the presence of physically and chemically protected zones.

[7] Along these lines, the primary objectives of this work are (1) to elucidate the controls of model structure on the system transit time and age distribution, and (2) to critically compare current soil biogeochemical models using these distributions. To address these two issues, we first present a range of models conceptually representing different biogeochemical processes and briefly review the theory of time-invariant linear impulse-response systems. Second, we compute transit times and age distributions for the different models, and describe the simulated responses to an external stochastic input. Finally, we focus on the mean transit time (which is proportional to the equilibrium soil organic matter content) and analyze how it is affected by changes in environmental conditions. Using a measure of the sensitivity of the mean transit time we discuss how different model formulations may lead to different responses to these environmental changes.

2. Methods

2.1. Models of Organic C Dynamics in Soils

[8] In this section, different approaches to model the long-term evolution of carbon in soils and plant residues are described. Figure 2 illustrates the model schemes and highlights the logical relationships among them. The same models will be analyzed in terms of their transit time and age distributions. Symbols and subscripts are defined in the notation section.

2.1.1. Discrete Models

[9] Most early soil biogeochemical models at the yearly timescale only considered a single organic matter compartment decomposing according to first-order kinetics, i.e., where organic matter is respired at a rate $O(t) = kx(t)$ [*Jenny*, 1941; *Olson*, 1963; *Trumbore*, 2000]. The corresponding mass balance equation is

$$\frac{dx(t)}{dt} = I(t) - kx(t), \tag{1}$$

where k is the linear decay rate, which depends on the chemistry of the substrate and on climatic factors (in particular soil moisture and temperature, here assumed to be represented by their long-term averages). Single compartment models are able to capture the general dynamics of litter decomposition and soil organic matter mineralization and are invoked for their simplicity. Obviously, they cannot account for the chemical heterogeneity of organic matter and the different decay rates in the early versus late stages of decomposition [*Andren and Paustian*, 1987]. For this reason, multicompartment models and continuous models have been developed. Three main model structures are generally employed: (1) parallel compartments, (2) series of compartments, and (3) feedback systems (Figure 2).

[10] *Minderman* [1968] was among the first to suggest that different organic compounds in plant residues decom-

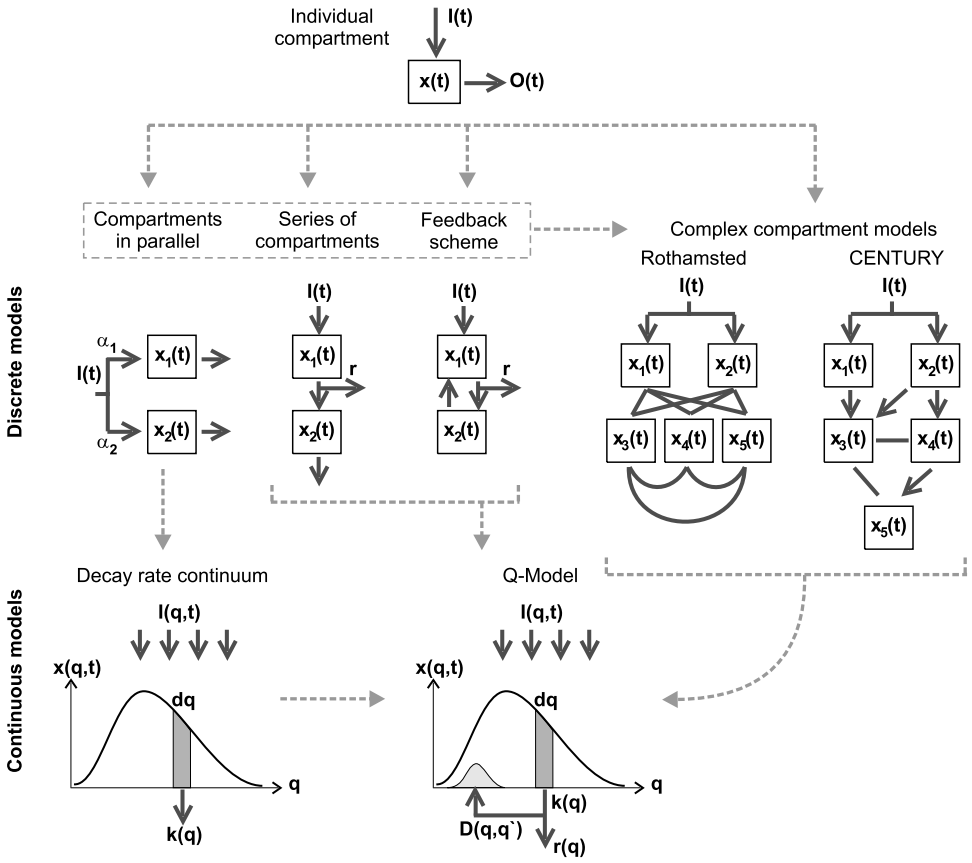

Figure 2. Schematic illustration of the different model structures. Thick solid lines represent carbon fluxes; dashed lines indicate how models are logically related in order of increasing generality. The schemes of Rothamsted [*Jenkinson and Rayner*, 1977] and CENTURY models [*Parton et al.*, 1987] have been simplified for clarity (thick solid lines without arrows indicate two-way flow; respiration losses from all compartments are not depicted). The continuous models employ a quality index q instead of discrete compartments, and the transfer between quality states is computed according to a dispersion function $D(q, q')$ [*Ågren and Bosatta*, 1996].

pose independently. This view was embedded in models based on parallel compartments, each representing a chemically homogeneous SOM fraction or a single litter type, and decomposing according to first-order kinetics [e.g., *Andren and Paustian*, 1987; *Bernoux et al.*, 1998; *Feng and Simpson*, 2008; *Zhang et al.*, 2007; *Hui and Jackson*, 2009]. In the simpler case of two parallel compartments, each fed by a fraction of the input (Figure 2) the system is described by the two independent equations,

$$\begin{cases} \dfrac{dx_1(t)}{dt} = \alpha_1 I(t) - k_1 x_1(t) \\ \dfrac{dx_2(t)}{dt} = \alpha_2 I(t) - k_2 x_2(t) \end{cases}, \tag{2}$$

where $\alpha_1 + \alpha_2 = 1$.

[11] The assumption that different compounds decompose independently can be relaxed considering a series of linear compartments (Figure 2). For example, this scheme approximates the process of assimilation of fresh organic matter by microbial decomposers (i.e., x_1), the turnover of which leads to humified compounds (x_2), and allows distinguishing the decomposition flux (i.e., the output from a compartment) from decomposer respiration (i.e., the fraction of that output that is lost to the atmosphere). A number of mathematical models based on this structure have been developed to simulate litter [*Andren and Paustian*, 1987] and SOM decomposition at spatial scales ranging from the soil core to the global scale [e.g., *Andren and Katterer*, 1997; *Bolin*, 1981; *Nicolardot et al.*, 2001]. A system of two compartments in series can be described by the coupled equations

$$\begin{cases} \dfrac{dx_1(t)}{dt} = I(t) - k_1 x_1(t) \\ \dfrac{dx_2(t)}{dt} = (1-r) k_1 x_1(t) - k_2 x_2(t) \end{cases}, \tag{3}$$

where k_1 and k_2 are the decay rates of the two compartments, and r is the fraction of the decomposed material that is respired during the transfer to the second compartment.

[12] When there are two-way interactions between the compartments, a feedback model can be used (Figure 2). These interactions arise during carbon exchange between unprotected (x_1) and physically protected pools (e.g., x_2 indicates C within soil aggregates or bond to clay particles that is exchanged through linear adsorption-desorption kinetics), or in substrate-decomposer systems, where

microbes (x_2) receive a flux from the substrate (x_1) and return carbon to the substrate through cell turnover [e.g., *Bosatta and Staaf*, 1982; *Bruun et al.*, 2004; *Manzoni and Porporato*, 2007]. The simplest feedback model with first-order kinetics can be represented as

$$\begin{cases} \dfrac{dx_1(t)}{dt} = I(t) + k_2 x_2(t) - k_1 x_1(t) \\ \dfrac{dx_2(t)}{dt} = (1-r)k_1 x_1(t) - k_2 x_2(t) \end{cases}, \tag{4}$$

where only the fraction $1-r$ of the output from the first compartment is fed to the second one.

[13] The simplified models in equations (1)–(4) have been increasingly replaced by complex multicompartment models [*Manzoni and Porporato*, 2009], in which different biogeochemical characteristics (e.g., decomposer biomass, labile or refractory organic matter) are associated with each compartment, arranged according to complex structures with several feedback loops, and both serial and parallel compartment arrangements. Here, we focus on two of the most frequently used soil C models, the Rothamsted [*Jenkinson*, 1990; *Jenkinson and Rayner*, 1977] and the CENTURY [*Parton et al.*, 1987, 1993] models (see Figure 2 for schematic representations of the two model structures). Both are based on a linear network of five organic matter compartments with different chemical and physical properties. Specifically, CENTURY has structural and metabolic pools for fresh residues, and active (including microbial biomass), slow, and passive compartments to describe soil organic matter (decay rates under optimal environmental conditions are 1/3, 2, 2/3, 1/25, and 10^{-3} yr^{-1}, respectively). Plant residues are split into the structural and metabolic pools and subsequently flow toward the active and slow SOM compartments, from which organic compounds reach the passive pool. In the Rothamsted model, plant residues are similarly split between decomposable and recalcitrant plant material, from which organic compounds are transformed into biomass, physically stable, and chemically stable SOM (decay rates are 4.2, 0.3, 0.41, 1.4×10^{-2}, 3.5×10^{-3} yr^{-1}, respectively). In both models, a fraction of C is respired at each passage between compartments, and partitioning coefficients regulate the flow toward more recalcitrant materials or feeding back to relatively labile pools. Thus, despite some differences in the way C is recycled among the more stable compartments, the two models are rather similar in terms of both structure and interpretation of the state variables.

2.1.2. Continuous Models

[14] Complex discrete models need a number of parameters to define all the fluxes and interactions among the pools. One way to reduce the number of parameters while maintaining a flexible model structure is to use continuous models, where the discrete compartments are substituted by a continuous quality index q [*Bosatta and Ågren*, 1985; *Carpenter*, 1981; *Tarutis*, 1994]. In this framework, organic compounds may be transferred between quality states or lost through respiration. The transfer across qualities is due to microbial assimilation at a given quality and return of byproducts and dead cells with a different decomposability [*Ågren and Bosatta*, 1996]. The system is thus conceptually similar to a series of compartments connected through decomposer activity, which redistributes matter along the series (Figure 2). In general, decomposition and respiration rates are functions of the substrate quality, resulting in a theoretical framework commonly referred to as Q-Model. The governing equation when decomposers are assumed to be instantaneously in equilibrium can be written as [*Ågren and Bosatta*, 1996],

$$\frac{\partial x_q(q,t)}{\partial t} = -\frac{u(q)}{1-r(q)} x_q(q,t) + \int_0^\infty D(q,q')u(q')x_q(q',t)dq', \tag{5}$$

where $x_q(q, t)$ is the amount of C at quality q and time t, $r(q)$ and $u(q)$ the quality-dependent respiration and microbial uptake rates, and $D(q, q')$ the probability density of a transition from quality q' to quality q during decomposer assimilation and decay. The input of organic matter is specified through the boundary conditions imposed on the problem. Since the model is linear, the effects of inputs at different times and qualities can be accounted for by summing up their different contributions. For an initial input at quality q_0, $I(q, 0) = \delta(q - q_0)$ (where δ denotes the Dirac delta function), equation (5) can be solved after specifying the initial condition $x(q, 0)$ and the functions $r(q)$, $k(q)$, and $D(q, q')$ [*Ågren and Bosatta*, 1996; *Bosatta and Ågren*, 2003]. Here, we consider a choice of the microbial functions that leads to analytical solutions and that has been extensively tested against observations (denoted as Model II in the work of *Bosatta and Ågren* [2003]).

[15] Note that, when the transition probability $D(q, q')$ and the initial input $I(q, 0)$ are combinations of Dirac delta functions (implying that the index q can only take a finite number of values), equation (5) can represent any discrete model. Thus, the Q-Model can be considered as a generalization of discrete compartment networks. In particular, when the decomposers do not change the quality of the substrate, i.e., $D(q, q') = \delta(q - q')$, the model (equation (5)) corresponds to a continuum of parallel linear compartments each decomposing according to an effective decay rate $k(q) = r(q)u(q)/[1 - r(q)]$ (Figure 2), which is a generalization of the parallel compartment model in equation (3) [*Ågren and Bosatta*, 1996; *Bosatta and Ågren*, 1995]. When this is the case, we can integrate both sides of equation (5) over the whole range of qualities and find a balance equation for the total C mass $x(t) = \int_0^\infty x_q(q, t)dq$ in the system,

$$\frac{dx}{dt} = -\int_0^\infty k(q)x_q(q,t)dq. \tag{6}$$

To solve equation (6), we consider a unitary input that is distributed across qualities according to the probability density function $x_q(q, 0)$. Since quality and decay rates are linked by the function $k(q)$, we will thereafter refer to the initial density distribution of decay rates as $p_k(k)$ for notational simplicity (note that $p_k(k)$ is analytically obtained from $x_q(q, 0)$ by means of a derived distribution). Models mathematically equivalent to equation (6) have been used in chemical engineering [*Aris*, 1989] and marine sediment biogeochemistry [*Boudreau and Ruddick*, 1991; *Rothman*

and Forney, 2007], but have been seldom applied to soil organic matter and plant residue decomposition [*Bolker et al.*, 1998; *Bosatta and Ågren*, 1995; *Forney and Rothman*, 2007].

[16] A typical choice for $p_k(k)$ is the gamma distribution, which is flexible enough to describe a variety of heterogeneous reactions [*Aris*, 1989; *Bolker et al.*, 1998; *Boudreau and Ruddick*, 1991; *Tarutis*, 1994],

$$p_k(k) = \frac{b^a}{\Gamma(a)} k^{a-1} \exp(-bk), \tag{7}$$

where the mean decay rate is $\mu_k = a/b$, and the variance is σ_k^2 $\sigma_k^2 = a/b^2$. Other choices for the distribution of decay rates are of course possible. Recently, *Forney and Rothman* [2007] described litter and soil organic matter decomposition assuming that $p_k(k)$ is a log-uniform distribution on the interval $\log a \leq \log k \leq \log b$,

$$p_k(k) = [(\ln b - \ln a)k]^{-1}. \tag{8}$$

Different distributions of decay rates $p_k(k)$ lead to a variety of behaviors in the temporal evolution of the mass and outflow of the soil system.

2.2. Input-Output Transformations and Transit Times

[17] Consider the previously described models as lumped input-output systems (Figure 1), where the inflow $I(t)$ is transformed into the outflow $O(t)$ depending on the internal properties of the system. In this long-term analysis, we assume that each transformation follows first-order kinetics and neglect the environmental effects on the decay constants, i.e., we focus on linear, time-invariant networks.

[18] The outflow $O(t)$ of any linear time-invariant system can be computed as a weighted sum of previous inputs [*Eriksson*, 1971; *Priestley*, 1999],

$$O(t) = \int_0^\infty \psi(T) I(t - T) dT. \tag{9}$$

The model-specific weighting function $\psi(T)$ describing the relative contribution of the input at previous time $t - T$ to the outflow at time t is the transit time distribution [*Nir and Lewis*, 1975]. $\psi(T)$ is also called transfer function or impulse response function [*Dingman*, 1994; *Priestley*, 1999]. If the input is impulsive (i.e., $I(t - T) = \delta(t - T)$), equation (9) yields $O(t) = \psi(t)$, i.e., the transit time distribution is equivalent to the temporal evolution of the output flux. Thus, for a linear system, the transit time distribution is the output flow resulting from an impulsive unitary input. Equation (9) is equivalent to a system of linear ODEs plus their initial conditions, and as such, it encompasses all the linear biogeochemical models described before. The form of the mass balance equations and their coefficient values determine the specific form of the function $\psi(T)$. Knowledge of the transit time distribution $\psi(T)$ gives a complete solution of the linear system through equation (9). In systems with high interannual climatic variability (e.g., dryland ecosystems) the assumption of time invariance of the kinetic constants may not hold. In these cases, the transit time distribution may vary in time and hence does not univocally characterize SOM dynamics [e.g., *Lewis and Nir*, 1978].

[19] It is mathematically convenient to work in the Laplace domain [*O'Neill*, 2003], which transforms the integral in equation (9) into an equivalent algebraic equation (convolution theorem [e.g., *Bechhoefer*, 2005; *Chen*, 2004; *Priestley*, 1999]),

$$\hat{O}(s) = \hat{\psi}(s)\hat{I}(s), \tag{10}$$

where carets and variable s denote Laplace transform.

[20] When the interest is in the system responses to inputs that fluctuate at different frequencies (ω), the Fourier transform of the transit time distribution is also employed. The Fourier transform $\hat{\psi}(\omega)$ is obtained by evaluating $\hat{\psi}(s)$ with $s = i\omega$ [*Bechhoefer*, 2005], where $i^2 = -1$, and $\hat{\psi}(\omega)$ becomes the frequency response function [*Chatfield*, 2004], or transfer function [*Bechhoefer*, 2005; *Priestley*, 1999]. For statistically stationary inputs (normalized to have zero mean), the square modulus of the transfer function, $|\hat{\psi}(\omega)|^2$, links the power spectrum of the output, $S_O(\omega)$, to the one of the input, $S_I(\omega)$ as [*Priestley*, 1999]

$$S_O(\omega) = |\hat{\psi}(\omega)|^2 S_I(\omega). \tag{11}$$

Equation (11) allows us to compute how the variance of the fluctuations in the input flux is redistributed by the system through its frequency response. When $|\hat{\psi}(\omega)|^2$ is decreasing with the frequency ω, the system acts as a low-pass filter, smoothing the oscillations; when it is increasing, the system enhances the higher frequencies and thus acts as a high-pass filter. Typically, networks of linear compartments dampen the input oscillations and increase the relative importance of the lower frequencies in the output (low-pass filter).

2.3. Age Distribution

[21] The exceedance probability of the transit time distribution $\psi(T)$ is the survivor function of the process,

$$A(\tau) = \int_\tau^\infty \psi(T) dT, \tag{12}$$

which represents the probability that a particle remains in the system for at least a time τ, i.e., its transit time is larger than τ. Accordingly, the total mass in the system $x(t)$ is computed by integrating the past input $I(t - \tau)$ weighted by the probability of remaining in the system for at least a time τ (i.e., $A(\tau)$, equation (12)), over the whole range of ages,

$$x(t) = \int_0^\infty I(t - \tau) A(\tau) d\tau. \tag{13}$$

When a unitary impulse input is applied, $I(t - \tau) = \delta(t - \tau)$ and equation (13) leads to $x(t) = A(t)$. Hence, the survivor function of the system is equal to the mass remaining at time t after an impulsive input.

[22] One can also define a density distribution of age τ at time t for the particles contained within the system, $\varphi(t, \tau)$.

The age distribution can be computed as the mass with age τ at time t (i.e., the amount entered at time $t - \tau$ that have transit times greater or equal to its age, see equation (12)) over the total mass at that time, $x(t)$. Using equation (13) the age distribution is readily obtained as

$$\varphi(t,\tau) = \frac{I(t-\tau)A(\tau)}{\int_0^\infty I(t-\tau)A(\tau)d\tau}. \quad (14)$$

When the temporal variability in the input is small, a steady state input flux can be assumed, i.e., $I(t - \tau) = I^*$. In this case, the total mass in the system is found from equation (13) as $x^* = I^*\overline{T}$, and equation (14) can be simplified to find a time-independent age density distribution $\varphi(\tau)$ as a function of the transit time exceedance probability $A(\tau)$ [*Bolin and Rodhe*, 1973; *Eriksson*, 1971; *Nir and Lewis*, 1975],

$$\varphi(\tau) = \frac{A(\tau)}{\int_0^\infty A(\tau)d\tau} = \frac{A(\tau)}{\overline{T}}. \quad (15)$$

For reasons of analytical tractability, we will mainly refer to this age distribution at steady state, $\varphi(\tau)$, and not to the time-dependent age distribution in equation (14). Equation (15) can be explained considering that at steady state, the probability of having an age between τ and $\tau + d\tau$ (i.e., $\varphi(\tau)d\tau$) is equal to the probability of having a transit time larger than τ. The latter is in turn the survivor function $A(\tau)$, suitably normalized by the mean transit time $\overline{T}$, to provide a probability density function.

[23] When the input temporal variability is important, the age distribution varies in time (equation (14)), while the transit time distribution $\psi(T)$ is still time-invariant and fully characterizes the output from the system. On the contrary, at steady state the age distribution does not provide any additional information on the system, because it is mathematically related to the transit time distribution (equations (12) and (15)).

[24] Nevertheless, both the steady state age distribution and the transit time distribution of SOM carbon are useful, since they reflect different soil properties. The age distribution describes how long molecules which are currently in the soil have resided there, while the transit time distribution describes how long outgoing molecules have been in the system. As such, they provide a complementary description of the system and can be used to interpret different available data (see section 3.3).

2.4. From the Individual Compartment to Network and Continuous Models

[25] The theory presented in sections 2.2 and 2.3 is now applied first to the individual-compartment model, and then to more complex networks of compartments and continuous models.

[26] The temporal evolution of the mass in an individual compartment (equation (1)) when an impulsive input of one unit of mass is applied and $x(t = 0) = 0$ is

$$x(t) = e^{-kt}, \quad (16)$$

and the corresponding output is $O(t) = kx(t)$. Since the outflow following a unitary impulsive input is equivalent to the transit time distribution we find

$$\psi(T) = ke^{-kT}, \quad (17)$$

with mean $\overline{T} = 1/k$. In the Laplace domain, equation (17) becomes

$$\hat{\psi}(s) = \frac{1}{1 + s/k}. \quad (18)$$

This result will be used to derive the transit time distribution in output fluxes from complex networks of individual linear compartments. By setting $s = i\omega$ in equation (18) we also find

$$|\hat{\psi}(\omega)|^2 = \frac{1}{1 + (\omega/k)^2}, \quad (19)$$

which can be used to compute the spectrum of the output flux following equation (11).

[27] When the system is at steady state, the age distribution can be easily computed from equation (15), as

$$\varphi(\tau) = ke^{-k\tau}, \quad (20)$$

with mean $\overline{\tau} = 1/k$. This is the only case where the age distribution is equal to the transit time distribution.

[28] The transit time and age distributions of more complex linear networks are found by combining the distributions of the individual building blocks (equations (17) and (20), respectively). This can be done by applying equation (10) and transforming the mass balance differential equations that control the system dynamics into an algebraic system in the Laplace domain [*Chen*, 2004]. The method, illustrated for the series of two compartments (equation (3)) in Appendix A, can similarly be applied to any linear time invariant network. In this manner, we computed analytical expressions for the density distributions $\psi(T)$ and $\varphi(\tau)$ for the models presented in section 2.1 (see Table 1 for details). In Table 1, we also reported the mean organic matter transit time $\overline{T}$ and the mean age $\overline{\tau}$ for each model.

[29] In models that use a distribution of decay rates (e.g., equations (7) and (8)), the transit time distribution can be obtained by applying the law of compound distributions [*Beck and Cohen*, 2003; *Benjamin and Cornell*, 1970; *Sornette*, 2004],

$$\psi(T) = \int_0^\infty \psi(k,T)p_k(k)dk. \quad (21)$$

In the simple case of an individual compartment with stochastic decay rate, $\psi(k, T)$ is given by equation (17), and, depending on the choices of the decay rate density distribution, equation (21) can lead to power law distributions of the whole-system transit times or ages (Table 1). In the Q-Model, we use the equivalence between the mass temporal evolution after an impulsive input and the age distribution (section 2.3), and directly use the solutions of

Table 1. Summary of Transit Time and Age Distributions and Their Mean for Different Model Structures[a]

Model	Transit Time Distribution $\psi(T)$	$\overline{T}$	Age Distribution $\varphi(\tau)$	$\overline{\tau}$
Individual compartment	ke^{-kT}	$\frac{1}{k}$	$ke^{-k\tau}$	$\frac{1}{k}$
Series of two compartments	$\frac{k_1\left[(1-r)k_2e^{-k_2T}-(k_2-k_1r)e^{-k_1T}\right]}{k_1-k_2}$	$\frac{(1-r)k_1+k_2}{k_1k_2}$	$\frac{k_1k_2\left[(1-r)k_1e^{-k_2\tau}-(k_2-k_1r)e^{-k_1\tau}\right]}{(k_1-k_2)[(1-r)k_1+k_2]}$	$\frac{1}{k_1}+\frac{1}{k_2}+\frac{1}{(1-r)k_1+k_2}$
Two compartments in parallel	$\alpha_1k_1e^{-k_1T}+(1-\alpha_1)k_2e^{-k_2T}$	$\frac{(1-\alpha_1)k_1+\alpha_1k_2}{k_1k_2}$	$\frac{k_1k_2\left[\alpha_1e^{-k_1\tau}+(1-\alpha_1)e^{-k_2\tau}\right]}{k_2\alpha_1+k_1(1-\alpha_1)}$	$\frac{1}{k_1}+\frac{1}{k_2}-\frac{1}{(1-\alpha_1)k_1+\alpha_1k_2}$
Feedback system[b]	$\frac{r(s+k_2)k_1}{(s+k_1)(s+k_2)-(1-r)k_1k_2}$	$\frac{(1-r)k_1+k_2}{rk_1k_2}$	$\frac{-rk_1k_2}{s[(1-r)k_1+k_2]}[1-\psi(s)]$	$\frac{(1-r)k_1(k_1+2k_2)+k_2^2}{rk_1k_2[(1-r)k_1+k_2]}$
Continuous model (gamma distribution of k)	$\frac{ab^a}{(b+T)^{a+1}}$	$\begin{cases}\frac{b}{a-1}, & a>1\\ \infty, & 0<a\le 1\end{cases}$	$\frac{(a-1)b^{a-1}}{(b+\tau)^a}$	$\begin{cases}\frac{b}{a-2} & a>2\\ \infty, & 0<a\le 2\end{cases}$
Continuous model (log-uniform distribution of k)[c]	$\frac{e^{-aT}-e^{-bT}}{T\ln(b-a)}$	$\frac{b-a}{ab\ln(b/a)}$	$\frac{ab}{(b-a)}[E_i(-b\tau)-E_i(-a\tau)]$	$\frac{b+a}{2ab}$

[a] See also Figures 2–5.
[b] The reported transit time and age distributions are left in the Laplace space for brevity.
[c] For the age distribution, $E_i(z)$ is the exponential integral function, defined as $E_i(z)=-\int_{-z}^{\infty}e^{-u}/u\,du$ [*Weisstein*, 2008].

equation (5) reported by *Bosatta and Ågren* [2003] to find $\varphi(\tau)$. Finally, $\psi(T)$ is obtained using equation (15).

3. Results and Discussion

[30] We investigated the effects of model structure on the shape of transit time and age distributions, and on the frequency response of the system in two distinct applications. First, we assume constant mean transit time to focus on the role of model structure and parameters on $\psi(T)$ and $\varphi(\tau)$ (section 3.1). In this way, the distributional properties of systems that are on average equivalent are compared. Second, we assess the sensitivity of the mean transit time (and thus the equilibrium soil C content) to changes in decay rates due to altered environmental conditions and litterfall quality (section 3.2).

3.1. Responses to Litterfall Input

[31] Figures 3–5 compare the responses of different models to an external input, assuming a common and constant mean transit time $\overline{T}$ for all models. The chosen example regards the forest floor of a Scots pine forest (detrended data from *Lehtonen et al.* [2008]), for which the assumption of constant $\overline{T}$ is reasonable because the decomposition rates of Scots pine needles tend to vary less than the litterfall input at the annual timescale [*Berg and McClaugherty*, 2003]. A constant mean transit time $\overline{T}$ = 3.5 years (estimated after *Berg and McClaugherty* [2003]) is assumed for all models by choosing the decay rate k_1 and setting constant values for the ratio k_1/k_2 and the remaining parameters r and α_1 (analytical expressions of $\overline{T}$ are reported in Table 1). The single compartment model, which is the building block of all the other model structures, is used as a baseline to assess the role of model architecture in shaping respiration flux, and transit time and age distributions. As shown in Figures 3–5 (dotted lines), its output flux is a simple low-pass filtered version of the input, resulting in lower variance of heterotrophic respiration compared to litterfall (i.e., lower area of the power spectrum of the outflow), and a faster decay of the respiration power spectrum ($S_O(\omega)\approx\omega^{-2}$) compared to the litterfall spectrum ($S_O(\omega)\approx\omega^0$, Figure 3d). In general, the higher the decomposition rate of the individual compartment (i.e., the lower the mean transit time), the closer the respiration flux is to the litterfall input. As a result, fast decay rates lead to weaker smoothing of the litterfall series and higher peaks of heterotrophic respiration.

[32] A similar filtering effect is also found using the other models considered in section 2.1. Figure 3 compares different versions of the parallel model (equation (2)), where chemically different compounds are decomposed independently. With this model, the response of the system to the litterfall input is proportional to the speed of the individual reactions (k_1 and k_2) and how the input is partitioned between the two compartments. When α_1 = 1 or 0, the system is equivalent to an individual compartment model. For $0<\alpha_1<1$, the system tends to be more reactive to litterfall than a single compartment because of the separation between a fast and a slow pool (dashed lines in Figures 3a and 3b). This results in respiration power spectra that are closer to the input spectrum (dashed line in Figure 3d), although the probability of long transit times increases as well. The transit time and age distributions of the parallel continuous model based on a gamma distribution of decay constants (equation (7) and Table 1) have heavier tails than typical discrete models (solid lines).

[33] In Figure 4, the series model is analyzed (equation (3)). When r = 1, the second compartment does not receive any input, so that the system becomes equivalent to an individual compartment. When r = 0, all decomposed compounds are transferred to the second compartment, from which they are respired. In this case, the system response to the litterfall input is delayed, as shown in Figures 4a and 4b (solid lines), and the mode of the transit time distribution is larger than zero. Intermediate values of respiration rate lead to relatively fast response of respiration to litterfall input, due to a high k_1 value, and long transit times due to the slower second compartment (dashed lines).

[34] Figure 5 illustrates the responses of the feedback model. The exchanges of mass between the mobile and the immobile phases increase the retention capacity of the system, as clearly shown by the longer transit times and ages compared to the individual compartment (solid and dashed lines in Figures 5b and 5c). The retention capacity

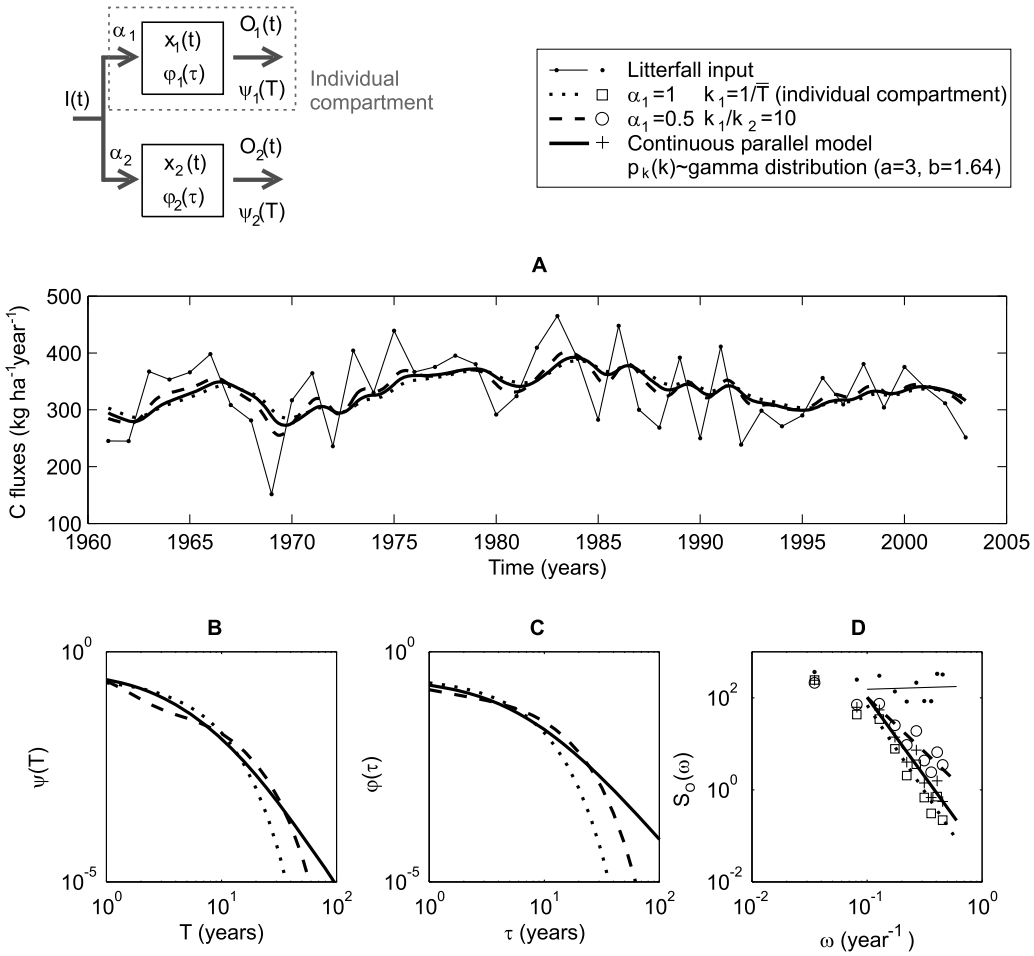

Figure 3. (top) Parallel compartment model (see equation (2)) and (bottom) effects of the partitioning coefficient α_1 on the simulated heterotrophic respiration fluxes and system response statistics, when $\overline{T}$ is the same for each parameter choice. (a) Comparison between litterfall [*Lehtonen et al.*, 2008] and respiration flux from equation (9); (b) transit time density distributions; (c) age density distributions, and (d) power spectra of litterfall and respiration, for different values of α_1 (equations are summarized in Table 1). The parallel compartment model is also compared with the continuous parallel model based on equation (7). In Figure 3d, a least squares fitting of the tails of the spectra with power law functions is also shown (lines).

however changes with the ratio k_1/k_2 when the whole system mean transit time is kept constant. If the second compartment releases mass at a slower rate than the first (in our example, $k_1/k_2 = 10$), the overall response is faster than in the case $k_1/k_2 = 1$ (Figures 5a and 5d).

[35] Figure 6 compares the transit times and age distributions of the individual compartment model to complex multicompartment and continuous quality models. Figure 6 shows that the individual compartment model has rapidly decaying transit time and age distributions, since it lacks the slowly turning compartments present in the Rothamsted [*Jenkinson and Rayner*, 1977] and CENTURY [*Parton et al.*, 1987]. These two more complex compartmental models show similar behavior, because of the relatively similar structure and values of the decay constants for the different compartments. Interestingly, when the original parameter values for optimal environmental conditions are used, both models had a mean transit time of ~25 years. Transit times and ages in the Q-Model decay with power law tails, in contrast with the other discrete models, which decay exponentially. Hence, the proportion of very old particles in the soil estimated by Q-Model is larger than that estimated from the compartment models. Since the Q-Model can be shown to be a generalization of the discrete multicompartment models [*Ågren and Bosatta*, 1996], it is not surprising that the two approaches lead to similar decay of the transit time distribution in the intermediate range of *T*.

3.2. Sensitivity of Mean Transit Time to Changes in Decay Rates

[36] In the previous section, we assessed the effects of model structure on the properties of the transit time and age distributions for constant mean transit time. We now explore how changes in the decay rates of the different SOM compartments affect the mean transit time $\overline{T}$. This analysis allows us to quantify the long-term C storage capacity of the soil, because under stationary conditions, $\overline{T}$ is a measure of the total soil organic C (recall that $x^* = I^*\overline{T}$,

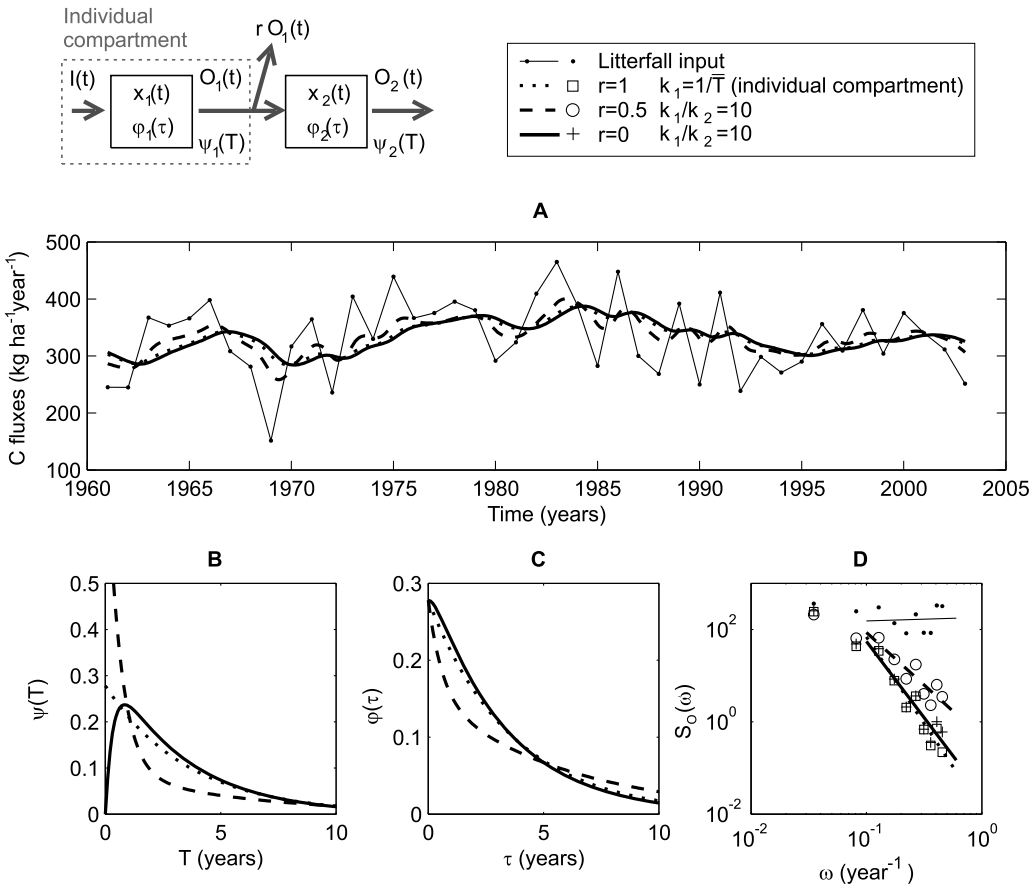

Figure 4. (top) Series of two compartments (see equation (3)) and (bottom) effects of respiration rate r on the simulated heterotrophic respiration fluxes and system response statistics, when $\overline{T}$ is the same for each parameter choice. (a) Comparison between litterfall and respiration flux from equation (9); (b) transit time density distributions; (c) age density distributions, and (d) power spectra of litterfall and respiration, for different values of r (equations are summarized in Table 1). In Figure 4d, a least squares fitting of the tails of the spectra with power law functions is also shown (lines).

from equation (13)). Faster decay rates in any of the compartments decrease $\overline{T}$, but the relative effect strongly depends on which compartment is considered, as shown in the following.

[37] To assess the responses of $\overline{T}$ to changes in a generic model parameter κ, we computed the sensitivity of the mean transit time as $\varepsilon = (\partial\overline{T}/\partial\kappa)/(\overline{T}/\kappa)$. This parameter indicates the relative change in mean transit time with respect to relative changes in the parameter κ and can be considered a dimensionless measure of the responsiveness (or elasticity) of the system. In this analysis, we focus on the effects of the decay constants, which are expected to change in response to altered climatic conditions [*Davidson and Janssens*, 2006] and as a consequence of shifts in species composition [*Cornwell et al.*, 2008]. In most models, the climatic effects are accounted for using a reduction function that decreases the maximum decay constant when temperature and soil moisture are below (or above) the optimal values [*Manzoni and Porporato*, 2007; *Rodrigo et al.*, 1997]. In contrast, shifts in species composition result in chemically different substrates, thus affecting the intrinsic decay rates.

[38] In general, an increase of the decay rate in any compartment is expected to yield a decrease in the mean transit time, i.e., $\varepsilon \leq 0$. The lower limit for ε can be computed when all decay constants in the model are changed proportionally, as assumed in most models [e.g., *Jenkinson*, 1990; *Parton et al.*, 1987, 1993; *Rodrigo et al.*, 1997]. In such a case, the response of the system is strongest and $\varepsilon = -1$ (as it can be easily proven for the single compartment model). Not all soil organic matter compartments, however, seem to respond equally [*Feng and Simpson*, 2008; *Giardina and Ryan*, 2000; *Knorr et al.*, 2005], so that $-1 < \varepsilon \leq 0$. Only when the change of a parameter does not alter significantly the mean transit time, is then ε equal to zero.

[39] For each of the simple discrete models (series, parallel, and feedback model) we computed the sensitivity to changes in k_1 for constant k_2 or vice versa. In this way, we can assess the effects of changes in the decay rate of one compartment, assuming the other is not affected. As shown in Figure 7a, the parallel model is more responsive (i.e., ε is more negative) when k_1/k_2 is low and k_2 is constant (solid lines), or when k_1/k_2 is high and k_1 is constant (dashed lines). This indicates that the strongest sensitivity occurs when the smaller decay constant is affected by climate while the fastest compartment is not affected. Larger α_1 (lighter

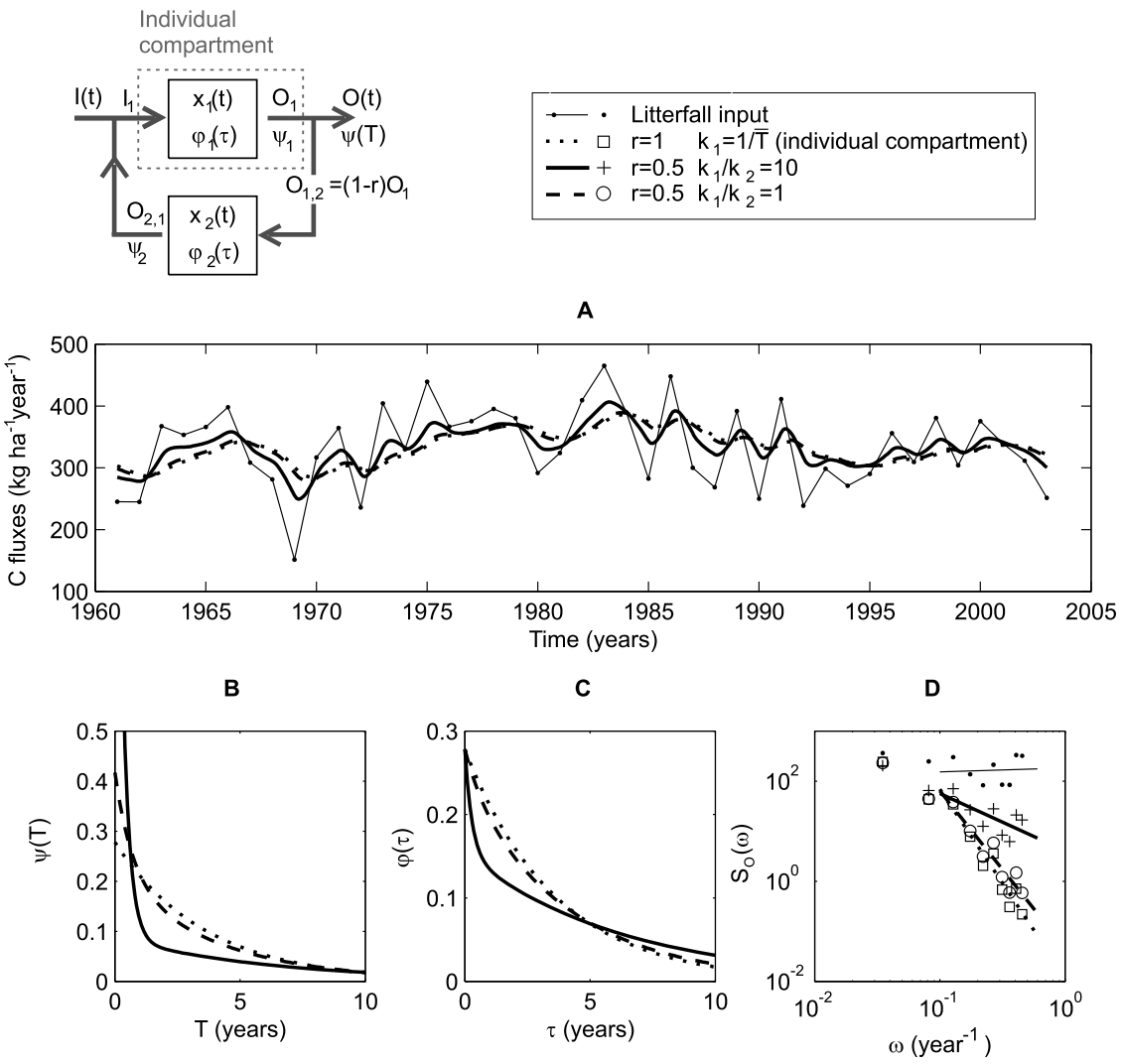

Figure 5. (top) Feedback model (see equation (4)) and (bottom) effects of the respiration rate r and the ratio k_1/k_2 on the simulated heterotrophic respiration fluxes and system response statistics, when $\overline{T}$ is the same for each parameter choice. (a) Comparison between litterfall and respiration flux from equation (9); (b) transit time density distributions; (c) age density distributions, and (d) power spectra of litterfall and respiration, for different values of r and the ratio k_1/k_2 (equations are summarized in Table 1). In Figure 5d, a least squares fitting of the tails of the spectra with power law functions is also shown (lines).

gray tones in Figure 7a) transfer most of the input to the first compartment in the parallel model (Figure 3), so that the system is more responsive (i.e., ε is more negative) to changes in k_1, and less to changes in k_2.

[40] A similar behavior characterizes the series and feedback models, as shown in Figure 7b (it is easy to show that these two models have the same analytical expression for ε). Similarly to the parallel model, in both series and feedback models the sensitivity is larger if the smaller decay constant is changed. Thus, if climatic changes or shifts in species composition affect the recalcitrant pools more than the labile ones, we can expect a stronger response. Higher respiration rates r (lighter gray tones in Figure 7b) make the system depend primarily on the dynamics of the first compartment, so that both models are more responsive to changes in k_1 at high r.

[41] Figure 7c illustrates how the sensitivity of the mean transit time changes as a function of the variability of the decay constant k in the continuous parallel model (equation (7)). Smaller variability in k (indicated by the coefficient of variation of the density distribution $p_k(k)$, σ_k/μ_k) results in stronger sensitivity to changes in both the mean decay constant μ_k (solid line in Figure 7c), and the variance σ_k^2 (dashed line).

3.3. Estimating Transit Times From Observations

[42] In this section, we discuss how the same mathematical framework previously described can also be used to infer model characteristics from observations. Two types of observations can be used: (1) C mass or respired CO_2 temporal evolution and (2) C isotope concentrations in SOM or CO_2 flux. In both cases, the proportionality between output flux and transit time distribution (section 2.2), and between C

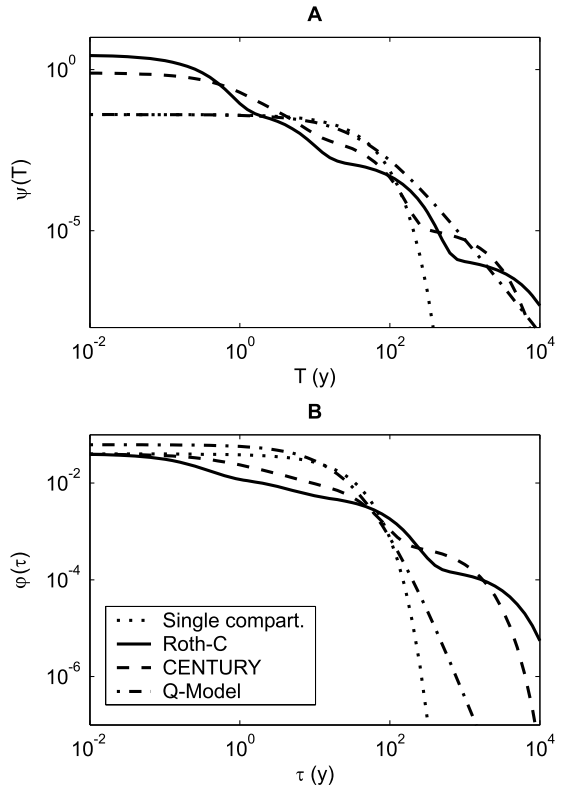

Figure 6. Comparison of (a) transit time and (b) steady state age distributions of different soil organic matter models. All parameters for Rothamsted [*Jenkinson and Rayner*, 1977] and CENTURY [*Parton et al.*, 1987] are from the original sources; the decay rate of the individual compartment model and decay rate at quality $q = 1$ in Q-Model are defined to have a mean transit time of 25 years.

mass and age distribution (section 2.3) after an impulsive input can be employed to link measurable quantities to the statistical properties of the soil system.

[43] The kinetic constants can be estimated by fitting the temporal evolution of C mass in litterbags or soil cores where the initial amount is known and the external inputs can be neglected [e.g., *Andren and Paustian*, 1987; *Forney and Rothman*, 2007; *Zhang et al.*, 2007]. Alternatively, in short-term laboratory experiments, the observed cumulative CO_2 outflow (i.e., $1 - A(\tau)$) can be used [e.g., *Nicolardot et al.*, 2001]. When studying larger systems at decadal or longer timescales, direct observation of soil C mass and fluxes becomes not feasible. A possible remedy is to use isotopic tracers to estimate the soil transit time and age distributions [*Balesdent*, 1987; *Bernoux et al.*, 1998; *Ehleringer et al.*, 2000; *Trumbore*, 2000]. The evolution of the mass of a tracer subject to simultaneous radioactive decay and mineralization according to the dynamics of the soil where it has been injected can be computed from a generalization of equation (13) [*Nir and Lewis*, 1975],

$$x_T(t) = \int_0^\infty I_T(t-\tau)A(\tau)e^{-\lambda\tau}d\tau, \qquad (22)$$

where $x_T(t)$ is the tracer mass, $I_T(t)$ the tracer input, and $e^{-\lambda\tau}$ a weighting function that accounts for radioactive decay at a constant rate λ.

[44] Typically, ^{13}C or ^{14}C are used. The concentration of ^{13}C in the input depends on the vegetation photosynthetic pathway, with C3 plants discriminating against ^{13}C more than C4 plants [*Bernoux et al.*, 1998]. ^{13}C is thus suitable to study long-term SOM changes where a transition from a C3- to a C4-dominated ecosystem occurred [*Bernoux et al.*, 1998; *Ehleringer et al.*, 2000]. ^{14}C concentration in the atmosphere, and consequently in vegetation and plant residues, has peaked in the early 1960s due to nuclear weapon testing and has steadily decreased thereafter. This strong signature in the input with respect to the SOM stock provides an opportunity to track SOM evolution at yearly to decadal timescales [*Trumbore*, 2000; *Bruun et al.*, 2005]. For both isotopes, the compound changes in atmospheric concentration, different discrimination by vegetation types, and variations in plant residue production determine the evolution of the tracer input $I_T(t)$.

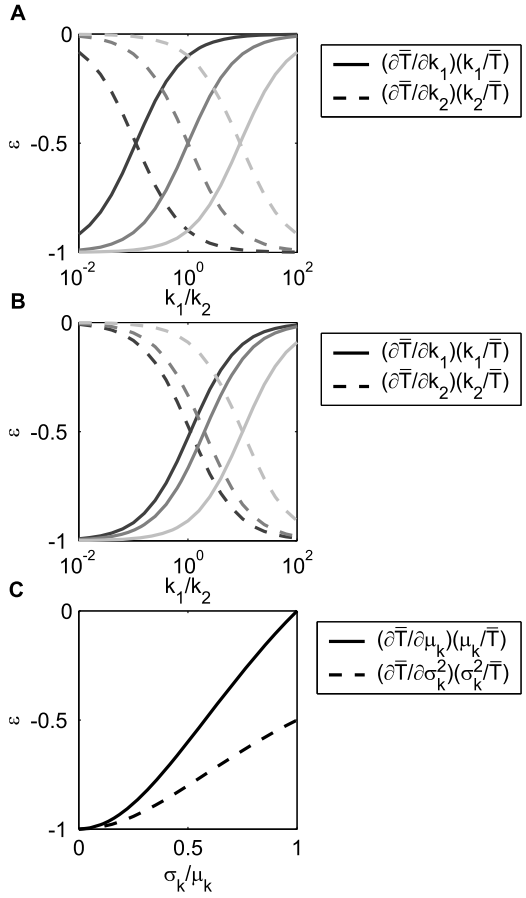

Figure 7. Sensitivity of the mean transit time (ε) to changes in decay rates. (a) Parallel model (lighter tones indicate increasing α_1 from 0.1 to 0.9); (b) series and feedback models (lighter tones indicate increasing r from 0.1 to 0.9). Solid lines represent sensitivity to changes in k_1 (with constant k_2), and dashed lines represent the sensitivity to changes in k_2 (with constant k_1). (c) Continuous parallel model, where ε is computed with respect to the mean and the variance of $p_k(k)$ (μ_k and σ_k^2, respectively; see equation (7)).

[45] When the mass $x_T(t)$ is measured, equation (22) can be used to infer the survivor function and thus, through linear system theory, the age and transit time distributions for the system (equations (12) and (15)). This approach has been employed to estimate the decay constants of individual compartment [*Balesdent*, 1987; *Bruun et al.*, 2005] and more complex multicompartment models [*Baisden et al.*, 2002; *Bruun et al.*, 2004]. It is important to note that the application of equation (22) to infer from tracer data the kinetic constants may be complicated by (1) occurrence of isotopic discrimination and (2) possible nonuniqueness of the solution to the inverse problem. If isotopic discrimination occurs during decomposition, the survivor functions for the different C isotopes is different. For example, the fraction of respired ^{13}C (parameter r in our framework) is likely smaller than the fraction of respired ^{12}C, inducing ^{13}C enrichment, while the initial fraction of ^{13}C in recalcitrant SOM (parameter α) is probably lower than the initial fraction of ^{12}C, leading to overall ^{13}C depletion in the respired flux [*Ågren et al.*, 1996; *Ehleringer et al.*, 2000]. The different values of these parameters translate in isotope-specific transit time and age distributions.

[46] Moreover, the inversion of equation (22) may lead to nonunique solutions in terms of kinetic constant values and shape of the survivor function. For example, the same SOM isotopic composition at a given time may be consistent with different kinetic constants so that individual isotope measurements are not sufficient to univocally determine k even for a single-pool model [*Trumbore*, 2000]. Also, the age distributions of different models are often similar (Figures 3–6). As a consequence, different model structures and input temporal evolutions might explain the same observed tracer concentrations [e.g., *Bruun et al.*, 2004]. For these reasons, when interpreting tracer data, the number of model parameters should be kept to a minimum [*Bernoux et al.*, 1998], and isotopic concentrations should be repeatedly measured through time (e.g., using archived soil samples [*Trumbore*, 2000]).

4. Conclusions

[47] We have shown that different model structures commonly employed to simulate soil biogeochemical processes can be analyzed using linear system theory. We derived the transit time and age distributions for each model structure, showing that the presence of feedback loops and parallel compartments with different decay rates tend to increase the retention of at least a fraction of organic matter particles in the soil. Models employing a continuum of decay rates lead to power law tails in both the transit time and the age distributions. Among the models that are currently used to simulate long-term soil C dynamics, the continuum quality Q-Model may give rise to this power law behavior, and thus predict higher organic matter retention than other linear multicompartment models (CENTURY and Rothamsted). We also found that the soil system tends to respond more strongly to altered climatic conditions (temperature or soil moisture in particular) when all the compartments are equally affected. However, experiments have highlighted that some compartments may be more sensitive to altered conditions than others. In such a case, the stronger sensitivity of the mean transit time is found in systems where the slower compartments are more sensitive and the rate of C losses from these slow pools is higher.

Appendix A: Computing the Transit Time Distribution in Series of Linear Compartments

[48] The system in equation (3) can be written in terms of the output fluxes (using equation (10)) in the Laplace domain as two coupled algebraic equations

$$\begin{cases} \hat{O}_1(s) = \hat{\psi}_1(s)\hat{I}(s) \\ \hat{O}_2(s) = \hat{\psi}_2(s)\left[(1-r)\hat{O}_1(s)\right], \end{cases} \tag{A1}$$

where the flux $(1 - r)\hat{O}_1(s)$ represents the input to the second compartment in the series. Equation (A1) leads to $\hat{O}_2(s) = (1 - r)\hat{\psi}_1(s)\hat{\psi}_2(s)\hat{I}(s)$. If we account for the losses from the first compartment (i.e., $r\hat{\psi}_1(s)\hat{I}(s)$), the total output from the system (symbols without subscript) becomes

$$\hat{O}(s) = [r\hat{\psi}_1(s) + (1-r)\hat{\psi}_1(s)\hat{\psi}_2(s)]\hat{I}(s), \tag{A2}$$

where the first term in the square brackets represents the losses from the first compartment, and the second the outflow from the second one. The whole system transit time distribution $\hat{\psi}(s)$ is thus computed as

$$\hat{\psi}(s) = \hat{\psi}_1(s)[r + (1-r)\hat{\psi}_2(s)]. \tag{A3}$$

The solution of equation (A3) in the time domain and the corresponding age distribution (from equation (15)) are reported in Table 1 and shown in Figure 4b.

[49] The simple two-compartment model of equation (3) can be easily extended to an arbitrary number of linear compartments in series. The simplest, analytically tractable extension is to N identical compartments with transit time distribution equal to $\hat{\psi}_1(s)$, and respiration rate r. In this case, the whole system transit time distribution is given by

$$\hat{\psi}(s) = \frac{kr + s[(1-r)\hat{\psi}_1(s)]^N}{kr + s}, \tag{A4}$$

the Laplace inverse of which is

$$\psi(T) = \frac{k^N(1-r)^{N-1}T^{N-1}e^{-kT} + kr(N-1)\Gamma[N-1, k(1-r)T]e^{-rkT}}{\Gamma(N)}, \tag{A5}$$

where $\Gamma(\cdot)$ is the Gamma function and $\Gamma(\cdot,\cdot)$ is the incomplete Gamma function. When respiration losses are negligible ($r \approx 0$), except for the last compartment of the series, we obtain a gamma distribution of transit times (e.g., the instantaneous unit hydrograph derived by *Nash* [1957]),

$$\psi(T) = \frac{k^N T^{N-1} e^{-kT}}{\Gamma(N)}. \tag{A6}$$

The corresponding age distribution at steady state can be computed using equation (15).

Notation

Carets and variables s and ω denote Laplace- and Fourier-transformed fluxes, respectively; asterisks indicate steady state conditions.

a, b	parameters for $p_k(k)$ (equations (7) and (8)).	
$A(\tau)$	survivor function.	
$D(q, q')$	probability density of a transition from q' to q (equation (5)).	
i	subscript indicating a generic subcompartment.	
$I(t)$, I^*	input flux	$[M][T]^{-1}$.
$I_I(t)$	input flux of tracer (equation (22))	$[M][T]^{-1}$.
k, k_i	first-order kinetics constant	$[T]^{-1}$.
$O(t)$, O_i	output flux (total flux, or from compartment i only)	$[M][T]^{-1}$.
$p_k(k)$	density distribution of decay rates (equations (7) and (8))	$[T]$.
q	substrate quality (equations (5) and (6)).	
r	fraction of respired carbon.	
$S_I(\omega)$, $S_O(\omega)$	nonnormalized spectral densities of input and output fluxes	$[M]^2[T]^{-1}$.
T, $\overline{T}$	generic and mean transit times (Figure 1)	$[T]$.
t	time of observation (Figure 1)	$[T]$.
$u(q)$	quality-dependent microbial uptake (equation (5))	$[T]^{-1}$.
$x(t)$, x^*	C mass in the system or subcompartment	$[M]$.
$x_q(q, t)$	C mass at a given quality q (equations (5) and (6))	$[M]$.
$x_I(t)$	tracer mass at time t (equation (22))	$[M]$.
α_1, α_2	partitioning coefficients in equation (2).	
ε	sensitivity of $\overline{T}$ to changes in parameter κ, $(\partial\overline{T}/\partial\kappa)/(\overline{T}/\kappa)$.	
μ_k	mean of $p_k(k)$ (equation (7))	$[T]^{-1}$.
λ	radioactive decay constant (equation (22))	$[T]^{-1}$.
σ_k^2	variance of $p_k(k)$ (equation (7))	$[T]^{-2}$.
τ, $\overline{\tau}$	generic and mean age of particles in the system (Figure 1)	$[T]$.
$\psi(T)$	transit time density distribution	$[T]^{-1}$.
$\varphi(\tau)$	steady state age density distribution (equation (15))	$[T]^{-1}$.
$\varphi(t, \tau)$	time-dependent age density distribution (equation (14))	$[T]^{-1}$.

[50] **Acknowledgments.** This work was supported in part by the Forest-Atmosphere Carbon Transfer and Storage (FACTS-1), funded by the U.S. Department of Energy, and by the U.S. Department of Agriculture (grant 58-6206-7-029). A.P. gratefully acknowledges the support of the Landolt and Cie visiting Chair "Innovative strategies for a sustainable future" at the École Polytechnique Fédérale de Lausanne (EPFL), Lausanne, Switzerland. We also thank G. Botter and one anonymous reviewer for constructive comments.

References

Ågren, G. I., and E. Bosatta (1996), *Theoretical Ecosystem Ecology: Understanding Element Cycles*, 234 pp., Cambridge Univ. Press, Cambridge, U. K.

Ågren, G. I., et al. (1996), Isotope discrimination during decomposition of organic matter: A theoretical analysis, *Soil Sci. Soc. Am. J.*, *60*, 1121–1126.

Andren, O., and T. Katterer (1997), ICBM: The introductory carbon balance model for exploration of soil carbon balances, *Ecol. Appl.*, *7*, 1226–1236, doi:10.1890/1051-0761(1997)007[1226:ITICBM]2.0.CO;2.

Andren, O., and K. Paustian (1987), Barley straw decomposition in the field—A comparison of models, *Ecology*, *68*, 1190–1200, doi:10.2307/1939203.

Aris, R. (1989), Reactions in continuous mixtures, *AIChE J.*, *35*, 539–548, doi:10.1002/aic.690350404.

Baisden, W. T., and R. Amundson (2003), An analytical approach to ecosystem biogeochemistry modeling, *Ecol. Appl.*, *13*, 649–663, doi:10.1890/1051-0761(2003)013[0649:AAATEB]2.0.CO;2.

Baisden, W. T., et al. (2002), A multi-isotope C and N modeling analysis of soil organic matter turnover and transport as a function of soil depth in a California annual grassland soil chronosequence, *Global Biogeochem. Cycles*, *16*(4), 1135, doi:10.1029/2001GB001823.

Balesdent, J. (1987), The turnover of soil organic fractions estimated by radiocarbon dating, *Sci. Total Environ.*, *62*, 405–408, doi:10.1016/0048-9697(87)90528-6.

Bechhoefer, J. (2005), Feedback for physicists: A tutorial essay on control, *Rev. Mod. Phys.*, *77*, 783–836, doi:10.1103/RevModPhys.77.783.

Beck, C., and E. G. D. Cohen (2003), Superstatistics, *Physica A*, *322*, 267–275.

Benjamin, J. R., and C. A. Cornell (1970), *Probability, Statistics, and Decision for Civil Engineers*, 684 pp., McGraw-Hill, New York.

Berg, B., and C. A. McClaugherty (2003), *Plant Litter. Decomposition, Humus Formation, Carbon Sequestration*, 286 pp., Springer, New York.

Bernoux, M., et al. (1998), The use of stable carbon isotopes for estimating soil organic matter turnover rates, *Geoderma*, *82*, 43–58, doi:10.1016/S0016-7061(97)00096-7.

Blanco-Canqui, H., and R. Lal (2004), Mechanisms of carbon sequestration in soil aggregates, *Crit. Rev. Plant Sci.*, *23*, 481–504, doi:10.1080/07352680490886842.

Bolin, B., (1981), *Carbon Cycle Modelling*, 390 pp., John Wiley, Hoboken, N. J.

Bolin, B., and H. Rodhe (1973), Note on concepts of age distribution and transit-time in natural reservoirs, *Tellus*, *25*, 58–62.

Bolker, B. M., et al. (1998), Linear analysis of soil decomposition: Insights from the CENTURY model, *Ecol. Appl.*, *8*, 425–439, doi:10.1890/1051-0761(1998)008[0425:LAOSDI]2.0.CO;2.

Bosatta, E., and G. I. Ågren (1985), Theoretical-analysis of decomposition of heterogeneous substrates, *Soil Biol. Biochem.*, *17*, 601–610, doi:10.1016/0038-0717(85)90035-5.

Bosatta, E., and G. I. Ågren (1995), The power and reactive continuum models as particular cases of the Q-theory of organic-matter dynamics, *Geochim. Cosmochim. Acta*, *59*, 3833–3835, doi:10.1016/0016-7037(95)00287-A.

Bosatta, E., and G. I. Ågren (2003), Exact solutions to the continuous-quality equation for soil organic matter turnover, *J. Theor. Biol.*, *224*, 97–105, doi:10.1016/S0022-5193(03)00147-4.

Bosatta, E., and H. Staaf (1982), The control of nitrogen turn-over in forest litter, *Oikos*, *39*, 143–151, doi:10.2307/3544478.

Boudreau, B. P., and B. R. Ruddick (1991), On a reactive continuum representation of organic-matter diagenesis, *Am. J. Sci.*, *291*, 507–538.

Bruun, S., et al. (2004), Estimating vital statistics and age distributions of measurable soil organic carbon fractions based on their pathway of formation and radiocarbon content, *J. Theor. Biol.*, *230*, 241–250, doi:10.1016/j.jtbi.2004.05.005.

Bruun, S., et al. (2005), Estimating turnover of soil organic carbon fractions based on radiocarbon measurements, *Radiocarbon*, *47*, 99–113.

Carpenter, S. R. (1981), Decay of heterogenous detritus—A general model, *J. Theor. Biol.*, *89*, 539–547, doi:10.1016/0022-5193(81)90026-6.

Chatfield, C. (2004), *The Analysis of Time Series: An Introduction*, 6th ed., 333 pp., CRC Press, Boca Raton, Fla.

Chen, C.-T. (2004), *Signals and Systems*, 424 pp., Oxford Univ. Press, New York.

Cornwell, W. K., et al. (2008), Plant species traits are the predominant control on litter decomposition rates within biomes worldwide, *Ecol. Lett.*, *11*, 1065–1071, doi:10.1111/j.1461-0248.2008.01219.x.

Davidson, E. A., and I. A. Janssens (2006), Temperature sensitivity of soil carbon decomposition and feedbacks to climate change, *Nature*, *440*, 165–173, doi:10.1038/nature04514.

Dingman, S. L. (1994), *Physical Hydrology*, 575 pp., Prentice-Hall, Upper Saddle River, N. J.

Ehleringer, J. R., et al. (2000), Carbon isotope ratios in belowground carbon cycle processes, *Ecol. Appl.*, *10*, 412–422, doi:10.1890/1051-0761(2000)010[0412:CIRIBC]2.0.CO;2.

Emanuel, W. R., et al. (1981), Modelling the circulation of carbon in the world's terrestrial ecosystems, in *Carbon Cycle Modelling*, edited by B. Bolin, pp. 335–353, John Wiley, Hoboken, N. J.

Enting, I. G. (2007), Laplace transform analysis of the carbon cycle, *Environ. Model. Softw.*, *22*, 1488–1497, doi:10.1016/j.envsoft.2006.06.018.

Eriksson, E. (1971), Compartment models and reservoir theory, *Annu. Rev. Ecol. Syst.*, *2*, 67–84, doi:10.1146/annurev.es.02.110171.000435.

Feng, X., and M. J. Simpson (2008), Temperature responses of individual soil organic matter components, *J. Geophys. Res.*, *113*, G03036, doi:10.1029/2008JG000743.

Forney, D. C., and D. H. Rothman (2007), Decomposition of soil organic matter from physically derived decay rates, *Eos Trans. AGU*, *88*(52), Fall Meet. Suppl., Abstract B41C-0646.

Giardina, C. P., and M. G. Ryan (2000), Evidence that decomposition rates of organic carbon in mineral soil do not vary with temperature, *Nature*, *404*, 858–861, doi:10.1038/35009076.

Hui, D. F., and R. Jackson (2009), Assessing interactive responses in litter decomposition in mixed species litter, *Plant Soil*, *314*, 263–271, doi:10.1007/s11104-008-9726-x.

Jenkinson, D. S. (1990), The turnover of organic-carbon and nitrogen in soil, *Philos. Trans. R. Soc. London, Ser. B*, *329*, 361–368, doi:10.1098/rstb.1990.0177.

Jenkinson, D. S., and J. H. Rayner (1977), The turnover of soil organic matter in some of the Rothamsted classical experiments, *Soil Sci.*, *123*, 298–305, doi:10.1097/00010694-197705000-00005.

Jenny, H. (1941), *Factors of Soil Formation: A System of Quantitative Pedology*, 281 pp., McGraw-Hill, New York.

Knorr, W., et al. (2005), Long-term sensitivity of soil carbon turnover to warming, *Nature*, *433*, 298–301, doi:10.1038/nature03226.

Lal, R. (2008), Carbon sequestration, *Philos. Trans. R. Soc. London, Ser. B*, *363*, 815–830, doi:10.1098/rstb.2007.2185.

Lehtonen, A., et al. (2008), Testing dependence between growth and needle litterfall in Scots pine-a case study in northern Finland, *Tree Physiol.*, *28*, 1741–1749.

Lewis, S., and A. Nir (1978), Tracer theory in geophysical systems in steady and non-steady state. 2. Non-steady state theoretical introduction, *Tellus*, *30*, 260–271.

Manzoni, S., and A. Porporato (2007), Theoretical analysis of nonlinearities and feedbacks in soil carbon and nitrogen cycles, *Soil Biol. Biochem.*, *39*, 1542–1556, doi:10.1016/j.soilbio.2007.01.006.

Manzoni, S., and A. Porporato (2009), Soil carbon and nitrogen mineralization: Theory and models across scales, *Soil Biol. Biochem.*, *41*, 1355–1379, doi:10.1016/j.soilbio.2009.02.031.

McGuire, K. J., and J. J. McDonnell (2006), A review and evaluation of catchment transit time modeling, *J. Hydrol. Amsterdam*, *330*, 543–563, doi:10.1016/j.jhydrol.2006.04.020.

Minderman, G. (1968), Addition, decomposition and accumulation of organic matter in forests, *J. Ecol.*, *56*, 355–362, doi:10.2307/2258238.

Nash, E. (1957), The form of the instantaneous unit hydrograph, *IAHS AISH Publ.*, *45*, 114–121.

Nauman, E. B. (2008), Residence time theory, *Ind. Eng. Chem. Res.*, *47*, 3752–3766, doi:10.1021/ie071635a.

Nicolardot, B., et al. (2001), Simulation of C and N mineralisation during crop residue decomposition: A simple dynamic model based on the C: N ratio of the residues, *Plant Soil*, *228*, 83–103, doi:10.1023/A:1004813801728.

Nir, A., and S. Lewis (1975), tracer theory in geophysical systems in steady and non-steady state. 1, *Tellus*, *27*, 372–383.

Olson, J. S. (1963), Energy storage and the balance of producer and decomposers in ecological systems, *Ecology*, *44*, 322–331, doi:10.2307/1932179.

O'Neill, P. V. (2003), *Advanced Engineering Mathematics*, 5th ed., 1344 pp., Thompson Brooks/Cole, Stamford, Conn.

Parton, W. J., et al. (1987), Analysis of factors controlling soil organic-matter levels in Great-Plains grasslands, *Soil Sci. Soc. Am. J.*, *51*, 1173–1179.

Parton, W. J., et al. (1993), Observations and modeling of biomass and soil organic-matter dynamics for the grassland biome worldwide, *Global Biogeochem. Cycles*, *7*, 785–809, doi:10.1029/93GB02042.

Priestley, M. B. (1999), *Spectral Analysis and Time Series*, 890 pp., Academic, San Diego, Calif.

Rinaldo, A., et al. (2006), Transport at basin scales: 1. Theoretical framework, *Hydrol. Earth Syst. Sci.*, *10*, 19–29.

Rodrigo, A., et al. (1997), Modelling temperature and moisture effects on C-N transformations in soils: Comparison of nine models, *Ecol. Modell.*, *102*, 325–339, doi:10.1016/S0304-3800(97)00067-7.

Rodriguez-Iturbe, I., and J. B. Valdes (1979), Geomorphologic structure of hydrologic response, *Water Resour. Res.*, *15*, 1409–1420, doi:10.1029/WR015i006p01409.

Rothman, D. H., and D. C. Forney (2007), Physical model for the decay and preservation of marine organic carbon, *Science*, *316*, 1325–1328, doi:10.1126/science.1138211.

Sardin, M., et al. (1991), Modeling the nonequilibrium transport of linearly interacting solutes in porous-media—A review, *Water Resour. Res.*, *27*, 2287–2307, doi:10.1029/91WR01034.

Schimel, J. P. (2001), Biogeochemical models: Implicit versus explicit microbiology, in *Global Biogeochemical Cycles in the Climate System*, edited by E. D. Schulze et al., 350 pp., Academic, San Diego, Calif.

Sornette, D. (2004), *Critical Phenomena in Natural Sciences*, 2nd ed., 528 pp., Springer, New York.

Tarutis, W. J. (1994), A mean-variance approach for describing organic-matter decomposition, *J. Theor. Biol.*, *168*, 13–18, doi:10.1006/jtbi.1994.1083.

Thompson, M. V., and J. T. Randerson (1999), Impulse response functions of terrestrial carbon cycle models: Method and application, *Global Change Biol.*, *5*, 371–394, doi:10.1046/j.1365-2486.1999.00235.x.

Trumbore, S. (2000), Age of soil organic matter and soil respiration: Radiocarbon constraints on belowground C dynamics, *Ecol. Appl.*, *10*, 399–411, doi:10.1890/1051-0761(2000)010[0399:AOSOMA]2.0.CO;2.

von Luetzow, M., et al. (2008), Stabilization mechanisms of organic matter in four temperate soils: Development and application of a conceptual model, *J. Plant Nutr. Soil Sci.*, *171*, 111–124, doi:10.1002/jpln.200700047.

Weisstein, E. W. (2008), Exponential Integral, in *MathWorld—A Wolfram Web Resource*, Wolfram Res, Champaign, Ill. (Available at http://mathworld.wolfram.com/ExponentialIntegral.html)

Zhang, C. F., et al. (2007), Modeling mass and nitrogen remaining in litterbags for Canadian forest and climate conditions, *Can. J. Soil Sci.*, *87*, 413–432.

G. G. Katul, Nicholas School of the Environment, Duke University, Box 90328, Durham, NC 27708, USA.

S. Manzoni and A. Porporato, Civil and Environmental Engineering Department, Duke University, Box 90287, Durham, NC 27708-0287, USA. (stefano.manzoni@duke.edu)